OIL LUBRICATED CYLINDRICAL JOURNAL BEARING ANALYSIS USING THE FINITE ELEMENT METHOD

Marco Túlio Corrêa de Faria
Universidade Federal de Minas Gerais, Av. Antônio Carlos, 6627 – Pampulha – Belo Horizonte - MG
mtcdf@uol.com.br

Fernando de Assis G. Correia
Zollern Transmissões Mecânicas S.A, Av. Manoel Inácio Peixoto, 2147 - 36771-000 - Cataguases - MG
fcorreia@zollern.com.br

Nathália Souza Teixeira
Universidade Federal de Minas Gerais, Av. Antônio Carlos, 6627 – Pampulha – Belo Horizonte - MG
nathysow@hotmail.com

Abstract. *This work presents the development of a finite element procedure for computation of static and dynamic performance characteristics of cylindrical journal bearings operating at several conditions. This procedure is used not only to evaluate the validity of simplified bearing theories, such as the infinitely short journal bearing theory, but also to render predictions for the most relevant bearing performance characteristics at concentric and eccentric journal positions. Curves of bearing load capacity, damping coefficients and stiffness coefficients are obtained for cylindrical journal bearings at several rotating speeds in order to provide subsides for the selection of the proper oil lubricated journal bearing.*

Keywords: *Journal Bearings, Cylindrical Journal Bearings, Short Journal Bearings, Finite Element Method.*

1. INTRODUCTION

The performance of industrial rotating machinery relies strongly on the efficient design of its shaft supporting bearings (Zeidan and Herbage, 1991). The technological advances on the design of fluid film bearings have given a strong impulse to the development of high performance turbomachinery (Zeidan, 1992). Very important requirements for the fluid film bearings employed on industrial turbomachinery are not only their capability of carrying efficiently the loads generated under stringent operating conditions and providing effectively means to stabilize the rotating machine under unexpected sources of dynamic forces, but also their long operating life (Knöss, 1980).

Lubricated journal bearings applied to industrial rotating machinery can basically be divided into two groups: fixed geometry and variable geometry bearings (Allaire and Flack, 1981). Of all feasible journal bearings designed for industrial rotating machinery, the fixed pad cylindrical journal bearing presents the simplest configuration and the lowest manufacturing costs (Hamrock, 1994).

The performance characteristics of cylindrical journal bearings are so important for mechanical engineering that several modern textbooks in mechanical design present technical data for their proper selection and design (Juvinall and Marshek, 1995; Shigley *et al.*, 2003; Norton, 2000). These technical data are generally based on approximate steady-state solutions for the classical Reynolds equation, which consists on the fundamental governing equation for fluid film journal bearings (Szeri, 1980). Furthermore, analytical procedures based on the simplified form of the Reynolds equation have been widely used to predict the bearing behavior on the preliminary design stages (San Andrés, 1989). Most of the practical solutions for oil-lubricated cylindrical journal bearings are based on the hypothesis of a bearing with infinite width (Sun, 1997).

The pioneer work of Reddi (1969) started the application of efficient finite element (FEM) procedures on the analysis of fluid film bearings. Since then, many efficient and accurate procedures have been devised to analyze the steady-state behavior of fluid film bearings (Booker and Huebner, 1972; Allaire *et al.*, 1977). However, the finite element prediction of the dynamic performance characteristics of oil-lubricated cylindrical journal bearings is very scarce in the technical literature (Faria *et al.*, 2006). The determination of the bearing steady-state performance characteristics, such as the load capacity and friction torque, and the dynamic characteristics, such as stiffness and damping force coefficients, are equally important for the development of safer, more efficient and more stable high speed rotating machinery (Childs, 1993).

This paper deals with a finite element procedure specially devised to analyze the static and dynamic behavior of fluid film cylindrical journal bearings. This procedure is capable of rendering both the steady-state and dynamic performance characteristics of journal bearings running under several operating conditions. The classical Reynolds equation is applied in conjunction with a linearized perturbation procedure (Klit and Lund, 1986) to generate the zero-th order and first order lubrication equations for the bearing, which serve to predict the bearing characteristics of interest. Firstly, the FEM procedure is used to evaluate the accuracy of some simplified bearing theories widely employed in the

design of journal bearings. Secondly, predictions of the bearing dynamic force coefficients are rendered by the FEM procedure in order to provide useful technical information about the bearing dynamic behavior. Several curves of bearing direct and cross-coupled stiffness synchronous coefficients and direct and cross-coupled damping synchronous coefficients are obtained to subsidize the proper selection of the bearing configuration for any rotating machinery.

2. JOURNAL BEARING PARAMETERS

Figure 1 depicts a schematic view of a cylindrical journal bearing with its geometrical and operating parameters. The basic geometric parameters are the bearing length L and diameter D. The journal bearing rotating speed is designated by Ω. The journal eccentricity, which is the distance between the journal center to the bearing center, can be written as e. The journal eccentricity components in the vertical and horizontal directions are given, respectively, by e_X and e_Y. The dimensionless journal eccentricity ratio is defined as $\varepsilon = e/c$, in which c represents the bearing radial clearance. The external load acting on the journal bearing is denoted by W. The bearing attitude angle, ϕ, is determined by $\phi = tan^{-1}(-F_Y/F_X)$, in which F_X e F_Y are the vertical and horizontal components of the bearing reaction force, respectively. The inertial reference frame is given by (X, Y, Z) and the rotating reference frame, which is attached to the journal, is represented by (x, y, z). The journal bearing kinematics is described by using the cylindrical coordinates R and θ. Hence, $x = R\theta$ and R is the journal radius.

(a) Journal bearing cross-section   (b) Side view of a journal bearing
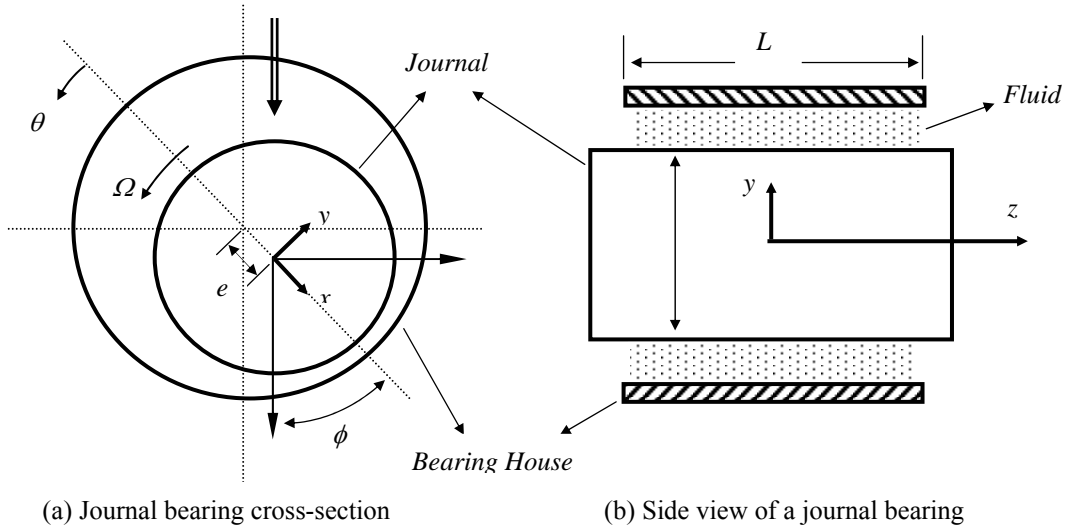
Figure 1. Transverse cross-section of a cylindrical journal bearing.

The thin fluid flow within the bearing clearance is described by the classical Reynolds equation. For isothermal flow of an incompressible fluid, the Reynolds equation can be expressed in cylindrical coordinates (θ, y, z) in the following form (Hamrock, 1994):

$$\frac{1}{R^2}\frac{\partial}{\partial\theta}\left(\frac{\rho h^3}{12\mu}\frac{\partial p}{\partial\theta}\right)+\frac{\partial}{\partial z}\left(\frac{\rho h^3}{12\mu}\frac{\partial p}{\partial z}\right)=\frac{1}{2}\frac{U}{R}\frac{\partial(\rho h)}{\partial\theta}+\frac{\partial(\rho h)}{\partial t} \tag{1}$$

in the flow domain given by $0\leq\theta\leq 2\pi$, $\frac{-L}{2}\leq z\leq\frac{L}{2}$. The journal surface velocity is represented by U ($U = \Omega R$). The hydrodynamic pressure, the dynamic fluid viscosity and the fluid mass density are given by p, μ e ρ, respectively. The bearing sides are at ambient pressure p_a, $p(\theta, L/2, t) = p(\theta, -L/2, t) = p_a$. The hydrodynamic pressure field is subjected to circumferential periodic boundary conditions, $p(\theta, z, t) = p(\theta+2\pi, z, t)$. The half Sommerfeld solution is employed in the computation of the pressure field (Hamrock, 1994). The thin fluid film thickness h is expressed as:

$$h = c + e_X(t)cos(\theta) + e_Y(t)sin(\theta). \tag{2}$$

3. LUBRICATION EQUATIONS

The steady-state and dynamic performance characteristics of cylindrical journal bearings can be predicted by solving the zeroth and first-order lubrication equations (Faria et al., 2006). In order to obtain these lubrication equations, a very small perturbation $(\Delta e_X, \Delta e_Y)$ is applied at excitation frequency (ω) on a steady-state equilibrium

position (e_{Xo}, e_{Yo}) of the journal (Klit and Lund, 1986). The perturbed form for the fluid film thickness is given in the following manner.

$$h = h_o + \left(\Delta e_X h_X + \Delta e_Y h_Y \right) e^{i\omega t} = h_o + \Delta e_\sigma h_\sigma e^{i\omega t} \; ; \; \sigma = X,Y \; ; i = \sqrt{-1} \tag{3}$$

where h_o is the steady-state or zeroth-order film thickness and $h_X = \cos(\theta)$, $h_Y = sin(\theta)$. The small perturbations on the fluid film thickness provoke variations on the hydrodynamic pressure field. Assuming a linear perturbation procedure, an expression for the perturbed pressure field can be written in similar form.

$$p(\theta,t) = p_o(\theta,t) + (\Delta e_X p_X + \Delta e_Y p_Y)e^{i\omega t} = p_o + \Delta e_\sigma p_\sigma e^{i\omega t} \tag{4}$$

where p_o and (p_X, p_Y) represent, respectively, the zeroth-order and first-order pressure fields. Inserting Eq.(3) and Eq.(4) into Eq.(1), the zeroth- and first-order lubrication equations can be obtained as follows.

$$\frac{1}{R^2} \frac{\partial}{\partial \theta} \left(\frac{\rho h_o^3}{12\mu} \frac{\partial p_o}{\partial \theta} \right) + \frac{\partial}{\partial z} \left(\frac{\rho h_o^3}{12\mu} \frac{\partial p_o}{\partial z} \right) = \frac{1}{2} \frac{U}{R} \frac{\partial(\rho h_o)}{\partial \theta} \tag{5}$$

$$\frac{1}{R^2} \frac{\partial}{\partial \theta} \left(\frac{3\rho h_o^2 h_\sigma}{12\mu} \frac{\partial p_o}{\partial \theta} + \frac{\rho h_o^3}{12\mu} \frac{\partial p_\sigma}{\partial \theta} \right) + \frac{\partial}{\partial z} \left(\frac{3\rho h_o^2 h_\sigma}{12\mu} \frac{\partial p_o}{\partial z} + \frac{\rho h_o^3}{12\mu} \frac{\partial p_\sigma}{\partial z} \right) =$$
$$\frac{1}{2} \frac{U}{R} \left[\frac{\partial(\rho h_\sigma)}{\partial \theta} \right] + i\omega \rho h_\sigma \tag{6}$$

The steady-state form of the Reynolds equation (Eq.(5)) permits to predict the two-dimensional hydrodynamic pressure field generated by the oil film in cylindrical journal bearings. Two-dimensional industrial lubrication problems do not have closed-form solution (Szeri, 1980; San Andrés, 1989). The finite element method (FEM) has been widely employed to develop accurate procedures to solve the Reynolds equation (Allaire *et al.*, 1977; Klit and Lund, 1986). However, approximate analytical solutions have been often used in the analysis and design of cylindrical journal bearings (San Andrés, 1997). These analytical solutions use simplifying assumptions based on the magnitude order of the bearing length to diameter ratio or slenderness ratio (*L/D*). The long bearing model, in which the axial flow is assumed very small, can provide accurate results for cylindrical journal bearings with $L \geq 2.D$, while the short bearing model, which assumes that the circumferential flow is very small, is capable of rendering accurate results for $L \leq 0.25$, provided that the journal eccentricity ratio is moderate (San Andrés, 1997; Szeri, 1987). The validity of the one-dimensional solutions depends on the capability of determining accurately the exact value of bearing slenderness ratio that will allow predicting reliable results for a given cylindrical journal bearing and in what operating conditions these results can be used.

4. FINITE ELEMENT MODELING

The two-dimensional thin fluid film domain is discretized by using four-node isopararemetric finite elements. The zeroth- and first-order pressure fields, given respectively by, p_o e p_σ, are interpolated over the element domain, Ω^e, through bilinear shape functions $\{\psi_i^e\}_{i=1,2,3,4}$ (Bathe, 1982).

$$p_o^e = \psi_i^e . p_{oi}^i \quad \text{e} \quad p_\sigma^e = \psi_i^e . p_{\sigma i}^e \qquad (i = 1,2,3,4 \; ; \sigma = X,Y). \tag{7}$$

For the finite element domain, Ω^e, the Galerkin method (Huebner et al., 1995) is employed to render the finite element equations associated with the zeroth- and first-order lubrication equations. The zeroth-order finite element equation, which is related to the steady-state form of the Reynolds equation given by Eq. (5), can be written for a finite element *e* as follows.

$$k_{ji}^e p_{oi}^e = f_j^e + q_j^e \; ; \; i,j=1,2,3,4 \tag{8}$$

where $k_{ji}^e = \iint\limits_{\Omega_e} \left(\frac{\rho h_o^3}{12\mu} \left(\frac{1}{R^2} \frac{\partial \psi_i^e}{\partial \theta} \frac{\partial \psi_j^e}{\partial \theta} + \frac{\partial \psi_i^e}{\partial z} \frac{\partial \psi_j^e}{\partial z} \right) \right).d\Omega_e$, $f_j^e = -\iint\limits_{\Omega_e} \frac{\Omega \rho h_o}{2} . \frac{\partial \psi_j^e}{\partial \theta} d\Omega_e$ e $q_j^e = \oint\limits_{\Gamma_e} \psi_j^e \dot{m}_n .d\Gamma_e$. The finite element boundary is represented by Γ_e and the normal fluid flow through the border is given by $\dot{m}_n$.

Similarly, the first-order finite element equation, which represents the perturbed form of the Reynolds equation given by Eq. (6), can be written as.

$$k^e_{\sigma_{ji}} p^e_{\sigma_i} = f^e_{\sigma_j} + q^e_{\sigma_j}$$ (9)

in which

$$k^e_{\sigma_{ji}} = \iint_{\Omega_e} \frac{\rho h_o^3}{12\mu} \left(\frac{1}{R^2} \frac{\partial \psi_i^e}{\partial \theta} \frac{\partial \psi_j^e}{\partial \theta} + \frac{\partial \psi_i^e}{\partial z} \frac{\partial \psi_j^e}{\partial z} \right) d\Omega_e,$$

$$f^e_{\sigma_j} = \iint_{\Omega_e} \left\{ \frac{-3\rho h_o^2 h_\sigma}{12\mu} \left(\frac{1}{R^2} \frac{\partial p_o}{\partial \theta} \frac{\partial \psi_j^e}{\partial \theta} + \frac{\partial p_o}{\partial z} \frac{\partial \psi_j^e}{\partial z} \right) + \frac{\Omega \rho h_\sigma}{2} \frac{\partial \psi_j^e}{\partial \theta} - i.\omega.\rho.h_\sigma.\psi_j^e \right\}.d\Omega_e$$

$$q^e_{\sigma_j} = \oint_{\Gamma_e} \psi_j^e.\dot{m}^e_{\sigma_n}.d\Gamma_e,$$

The first-order normal fluid flow through the border Γ_e of a finite element is denoted by $\dot{m}_{\sigma_n}$.

5. STATIC AND DYNAMIC PERFORMANCE CHARACTERISTICS

The global zeroth-order finite element equation, defined over the entire thin fluid film domain Ω, is obtained by superposing the equations provided by Eq. (8). The solution of the zeroth-order lubrication equation leads to the steady-state hydrodynamic pressure field, which can be integrated over the fluid domain to render the bearing load capacity and other static performance characteristics, such as the friction torque and the side flow rate. The fluid film reaction forces can be estimated by the following expression, in which the ambient pressure is given by p_a.

$$F_{\sigma_o} = \int_0^L \int_0^{2\pi} (p_o - p_a)h_\sigma R.d\theta.dz ; \quad \sigma = X,Y.$$ (10)

The computation of the perturbed or first-order pressure field is performed by a system of complex finite element equations obtained from Eq. (9). The numerical integration of the first-order pressure field renders an estimate for the fluid film complex impedances $\{ Z_{\sigma\beta_o} \}_{\beta,\sigma=X,Y}$. The linearized stiffness coefficients, $\{ K_{\sigma\beta} \}_{\beta,\sigma=X,Y}$, and damping coefficients, $\{ C_{\sigma\beta} \}_{\beta,\sigma=X,Y}$, associated with the fluid film hydrodynamic action, assuming a shaft perfectly aligned, can be computed as follows.

$$Z_{\sigma\beta} = K_{\sigma\beta} + i\omega C_{\sigma\beta} = -\int_0^L \int_0^{2\pi} p_\beta h_\sigma R.d\theta.dz, \quad \beta,\sigma = X,Y$$ (11)

or

$$\begin{bmatrix} K_{XX} & K_{XY} \\ K_{YX} & K_{YY} \end{bmatrix} + i.\omega. \begin{bmatrix} C_{XX} & C_{XY} \\ C_{YX} & C_{YY} \end{bmatrix} = -\int_0^L \int_0^{2\pi} \begin{bmatrix} p_X h_X & p_Y h_X \\ p_X h_Y & p_Y h_Y \end{bmatrix} .R.d\theta.dz .$$ (12)

The synchronous dynamic force coefficients are computed at $\omega = \Omega$.

6. NUMERICAL RESULTS

This section is divided into three items: 1. Mesh size sensitivity analysis of the FEM procedure; 2. Evaluation of the theory of infinitely short journal bearing; 3. Performance analysis of cylindrical journal bearings. The second item is designed to evaluate how important is to determine exactly the bearing slenderness ratio (*L/D*) before using a simplified bearing theory to analyze cylindrical journal bearings. In the third item, some cylindrical journal bearing dynamic performance characteristics are estimated under several operating conditions.

6.1. Mesh size sensitivity analysis

An example of cylindrical journal bearing, whose parameters are shown on Tab. 1, is selected to evaluate the influence of the mesh size on the FEM estimates of bearing load capacity and direct stiffness coefficients. The data

provided by Tab. 1 are related to two cylindrical journal bearings that were specially designed for a horizontal rotor test rig (Faria *et al.*, 2005). The slenderness ratio of these bearings is equal to 0.8.

Figure 2 depicts the curves of dimensionless load capacity and direct synchronous stiffness coefficients for the bearing described on Tab. 1. The results presented on Fig. 2 permit to say that 400 finite elements represent a reasonable mesh size to guarantee numerical accuracy in the computation of bearing load and stiffness coefficients. The following expressions are employed as denominators to render the dimensionless bearing parameters shown on Fig. 2.

$$F^* = (p_a.L.D) \quad \text{and} \quad K^* = (p_a.L.D)/c \tag{13}$$

Table 1. Bearing parameters for the mesh sensitivity analysis.

$L = 0.012$ m	$\rho = 892$ kg/m^3
$D = 0.015$ m	$c = 34.5 \times 10^{-6}$ m
$\mu = 25$ mPa.s	Mesh size (number of circumferential elements multiplied by the number of axial elements)
$\Omega = 5,000$ rpm	
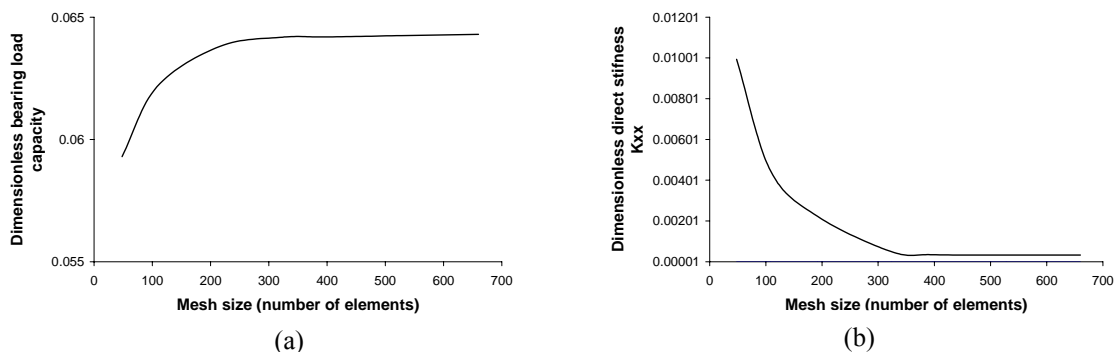
Figure 2. Curves of bearing performance characteristics versus the finite element mesh size: (a) curve of dimensionless bearing load capacity; (b) curve of dimensionless direct synchronous stiffness coefficients.

6.2. Evaluation of the short journal bearing theory

Primarily as an example of validation, curves of the journal eccentricity ratio in function of the Sommerfeld number are rendered by the short journal bearing (JB) theory and by the FEM procedure for comparison with results available on the technical literature (Shigley *et al.*, 2003; Norton, 2000; Juvinall and Marshek, 1995). These curves are presented for two values of slenderness ratio (*L/D*), which are 0.25 and 1. According to the classical Lubrication theory literature (San Andrés, 1997; Szeri, 1987), the ratio *L/D* = 0.25 is recommended as upper bound slenderness ratio for the short JB theory. The Sommerfeld number is a dimensionless parameter that combines geometric and operating bearing parameters expressed by

$$S = \frac{R^2}{c^2}.\mu.\frac{N}{P} \tag{14}$$

where *P* represents the bearing unit load, given by *P* = *F*/(*L.D*), and *N* represents the journal speed in Hz.

Figure 3 depicts the values of the journal eccentricity ratio versus the Sommerfeld number, for the slenderness ratio (*L/D*) of 0.25, predicted by the short JB theory (dashed line with triangles) and by the FEM procedure (dashed line with squares) comparatively to the data available in the technical literature (solid line). 1080 finite elements are employed to model the thin fluid film in the FEM procedure. It can be noticed that the pattern of the curve obtained by the short JB theory for *L/D* = 0.25 does not follow the patterns presented by the other two curves. Within the usual design range of Sommerfeld numbers, from 0.1 to 2, the short JB theory renders values of eccentricity ratios much higher than those currently used in the design of cylindrical journal bearings, even at *L/D* = 0.25. At low Sommerfeld numbers, the short JB theory predicts reasonably the values of eccentricity ratio. On the other hand, the agreement between the FEM predictions and the data available on the technical literature is very reasonable, and the average relative deviation is about 8.5 %.

The comparative values of eccentricity ratio are also computed for the slenderness ratio (*L/D*) of 1. Industrial oil-lubricated cylindrical journal bearings generally present values of slenderness ratio close to 1 (Allaire and Flack, 1981). Figure 4 shows the curves obtained by the FEM procedure (dashed line with squares) and by the short JB theory (dashed line with triangles) comparatively to the curve available on the technical literature (solid line). Again, the

values of eccentricity ratio predicted by the short JB theory are far from those presented in the technical literature (Shigley *et al.*, 2003; Norton, 2000; Juvinall and Marshek, 1995), except for very high Sommerfeld numbers. For $L/D = 1$, this poor agreement between the short JB theory and the technical literature is expected within the usual design range of Sommerfeld numbers. On the other hand, the average relative deviation between the FEM predictions and the data available on the technical literature is about 11.8 %. Furthermore, the FEM curve pattern matches well the pattern presented by the curve from the technical literature.
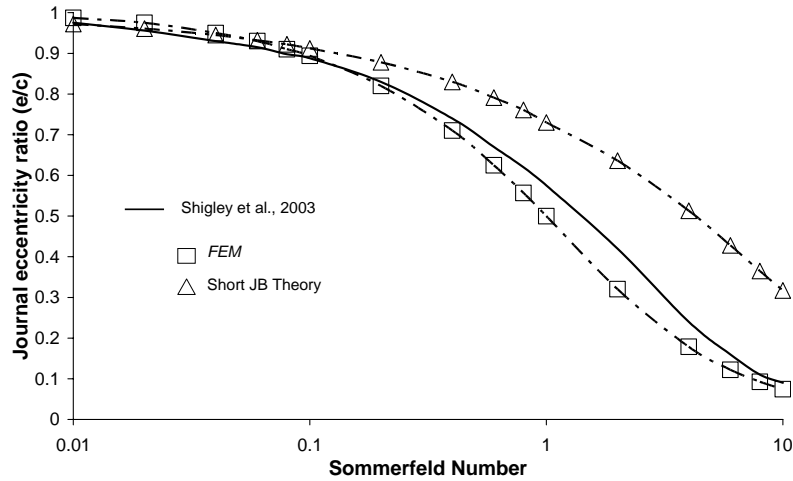
Figure 3. Comparative curves of journal eccentricity ratio versus Sommerfeld number for $L/D = 0.25$ (Solid line represents the technical literature data and the dashed lines represent the predictions computed by the FEM procedure and by the short JB theory).
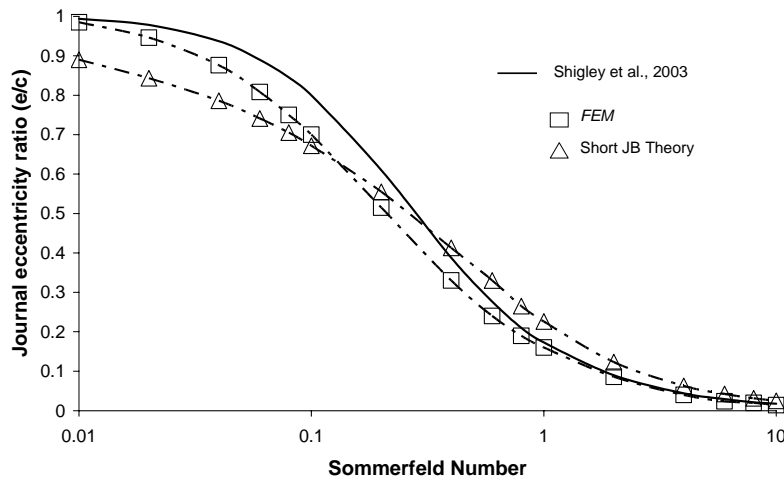
Figure 4. Comparative curves of journal eccentricity ratio versus Sommerfeld number for $L/D = 1$ (Solid line represents the technical literature data and the dashed lines represent the predictions computed by the FEM procedure and by the short JB theory).

Now, some cases of oil-lubricated journal bearings with small slenderness ratios are analyzed in order to assess the conditions at which the short JB theory is able to render accurate results for the bearing performance characteristics. The bearing load capacity and the dynamic force coefficients are computed for cylindrical journal bearings with different slenderness ratios by the FEM procedure and by the short JB theory. The bearing baseline parameters used are those given in Table 1. The bearing performance characteristics are evaluated at a wide range of rotating speeds (1,000 rpm to 10,000 rpm) and for several loading conditions (eccentricity ratios ranging from 0.01 to 0.9). The results obtained by the FEM procedure and by the short JB theory do not agree well, mainly for the bearing dynamic force coefficients. However, the predictions for the bearing load capacity are in the same of order of magnitude. Consequently, the comparative analysis of the short JB theory is performed using only the results obtained for the steady-state performance characteristic evaluated, which is the bearing carrying-load capacity.

Figure 5 depicts the comparative values of bearing load capacity predicted by the FEM procedure (solid lines) and by the short JB theory (dashed lines) at different load conditions (six eccentricity ratios). The curves are plotted against

the slenderness ratio (*L/D*) at the rotating speed of 5,500 rpm. The curve patterns are basically the same at any rotating speed. 4080 finite elements are employed in the thin fluid film geometric modeling (80 circumferential and 51 axial elements).
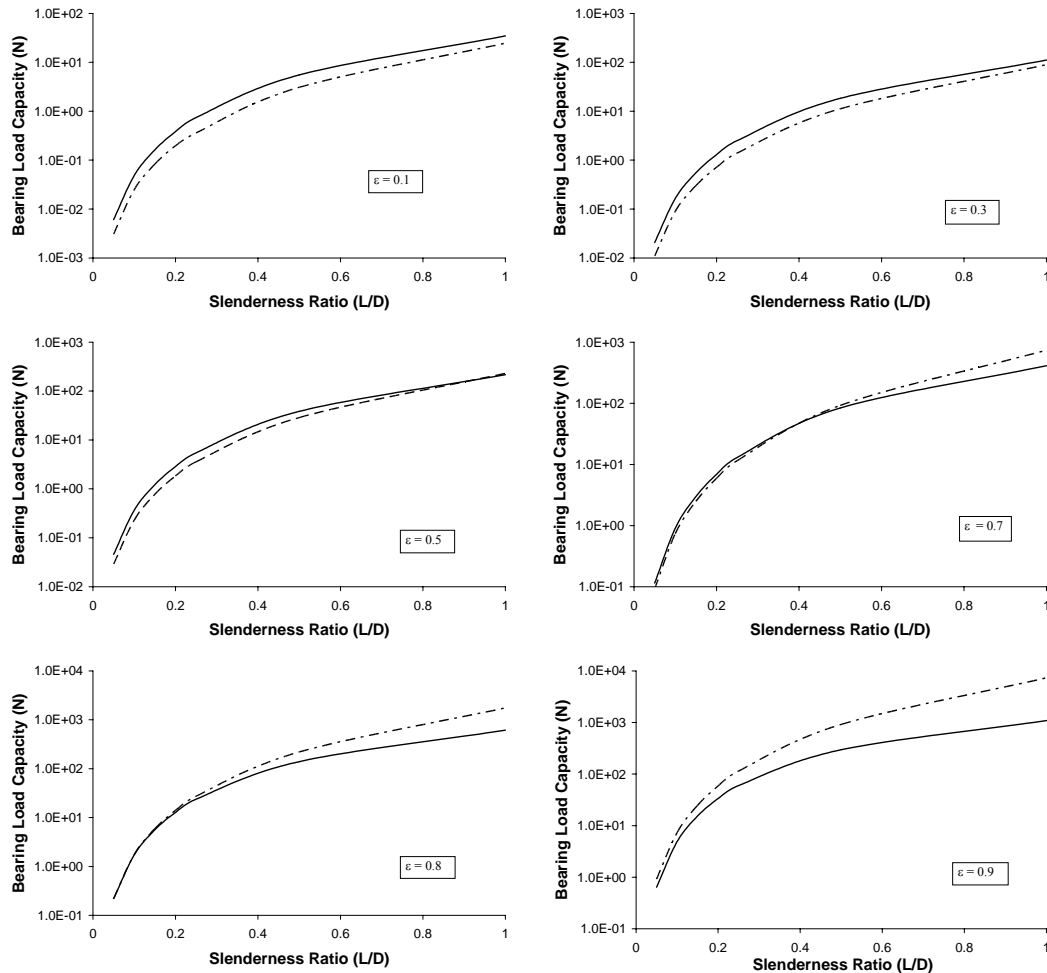
Figure 5. Comparative predictions of bearing load capacity versus the slenderness ratio for six eccentricity ratios, at the speed of 5,500 rpm. The solid lines represent the FEM predictions and the dashed lines the short JB theory predictions.

From the curves presented on Fig. 5, it can be seen that the short JB theory renders predictions of bearing load capacity in good agreement with those rendered by the FEM procedure for large eccentricity ratios ($0.7 \leq \varepsilon \leq 0.8$) and small slenderness ratios ($L/D \leq 0.25$). The curve patterns depicted on Fig. 5 coincide with that provided by the Lubrication theory technical literature (San Andrés, 1997; Szeri, 1987). Table 2 summarizes the results depicted on Fig. 5, providing the relative deviations between the FEM predictions and the short JB theory predictions obtained at six journal eccentricity ratios. This table corroborates with the classical Lubrication theory, showing clearly that the short JB theory is very appropriate for cylindrical journal bearings with $L/D \leq 0.25$, operating under moderate and high loads ($0.7 \leq \varepsilon \leq 0.8$).

Another example of bearing load computation at $L/D = 0.25$ is summarized on Figure 6, which depicts the comparative values of load capacity computed by the FEM procedure (solid lines) and by the short JB theory (dashed lines) for five eccentricity ratios. The bearing parameters used to generate Fig. 6 are given in Tab. 1. The finite element mesh uses 1080 elements. The average relative deviation between the FEM predictions and the short JB theory predictions is about 15.82% for $\varepsilon = 0.8$. At $\varepsilon = 0.55$, the average relative deviation reaches 30.57%. Again, the results show that the short JB theory can render acceptable values of load capacity for bearings operating under high loads ($\varepsilon = 0.8$) with $L/D = 0.25$.

Table 2. Relative deviation between the FEM predictions and the short JB theory predictions.

L/D	ε = 0.1	ε = 0.3	ε = 0.5	ε = 0.7	ε = 0.8	ε = 0.9
0.05	49.50%	46.96%	37.16%	19.93%	0.82%	43.17%
0.1	48.56%	45.52%	37.28%	18.54%	1.62%	50.11%
0.15	49.14%	45.47%	36.60%	16.75%	5.19%	60.89%
0.2	48.70%	44.97%	35.73%	14.35%	9.95%	74.92%
0.25	51.56%	44.29%	34.54%	11.43%	15.80%	91.69%
average	**49.49%**	**45.44%**	**36.26%**	**16.20%**	**6.67%**	**64.16%**
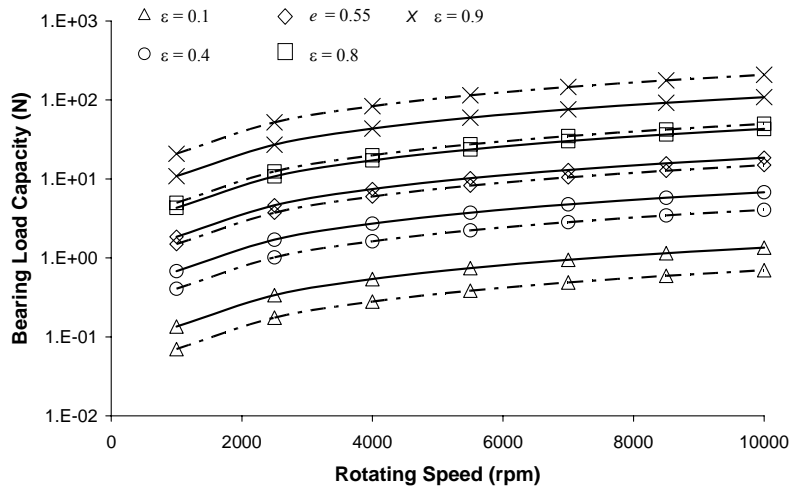
Figure 6. Comparative values of bearing load capacity computed by the FEM procedure (solid lines) and by the short JB theory (dashed lines) versus rotating speed at $L/D = 0.25$.

6.3. Dynamic force coefficients for cylindrical journal bearings

Curves of synchronous dynamic force coefficients are obtained for the bearing described on Tab. 1. In this case, the slenderness ratio (L/D) is equal to 0.8. The dimensionless values of stiffness and damping coefficients are computed using the following denominators

$$K^* = (p_a.L.D)/c \quad \text{e} \quad C^* = (p_a.L.D)/(c.\Omega) \tag{15}$$

where p_a represents the ambient pressure.

Figure 7 depicts the curves of dimensionless direct (K_{xx} and K_{yy}) and cross-coupled (K_{xy} and K_{yx}) stiffness coefficients versus eccentricity ratio at three journal rotating speeds. It is observed that the bearing becomes stiffer as the journal eccentricity ratio increases. Also, if the journal rotating speed increases, the bearing synchronous stiffness coefficients increase. The curves of the direct coefficients K_{xx} and K_{yy} versus the eccentricity ratio basically follow the same increasing pattern, although they use different graphical scales. The cross-coupled coefficient (K_{yx}) has opposite sign to that of the coefficient (K_{xy}).

The curves of synchronous dimensionless damping coefficients versus the eccentricity ratio are shown on Fig. 8. As the eccentricity ratio increases, the fluid viscous dissipating effects increase, as expected. Moreover, the fluid resistance, which is measured by the damping coefficients, increases as the rotating speed increases. Figure 8 shows the increasing trend of the bearing damping coefficients as either the eccentricity ratio increases or the rotating speed increases.
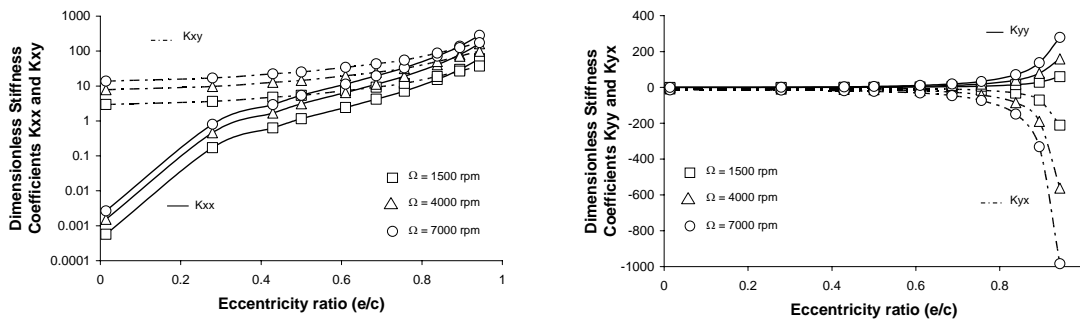
Figure 7. Curves of dimensionless synchronous direct stiffness coefficients [K_{xx} and K_{yy} (solid lines)] and cross-coupled coefficients [K_{xy} and K_{yx} (dashed lines)] varying with the eccentricity ratio for three rotating speeds.
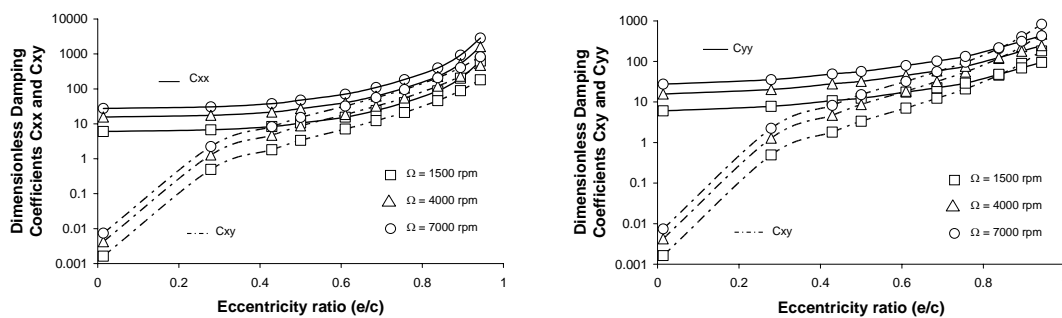
Figure 8. Curves of dimensionless synchronous direct damping coefficients [C_{xx} and C_{yy} (solid lines)] and cross-coupled coefficients [C_{xy} and C_{yx} (dashed lines)] varying with the eccentricity ratio for three rotating speeds.

7. CONCLUSIONS

The numerical results presented in this work show that the computational procedure developed for oil-lubricated cylindrical journal bearings presents a very satisfactory performance in the steady-state analysis of journal bearings. Moreover, the predictions obtained for the dynamic force coefficients at several operating conditions can provide important subsides for the preliminary design stages of fluid film bearings used in industrial rotating machinery.

The use of simplified bearing theories, as the infinitely short journal bearing (JB) theory, must be carefully evaluated in the analysis and design of cylindrical journal bearings. The short JB theory can introduce large errors in the computation of both steady-state and dynamic performance characteristics of cylindrical journal bearings, whose slenderness ratio (*L/D*) is generally close to 1. It is noteworthy to say that the development of efficient computational procedures for bearing analysis, such as the finite element procedure presented in this work, is extremely important for the design of safe, durable and efficient fluid film journal bearings.

8. REFERENCES

Allaire, P., Nicholas, J. and Gunter, E., 1977, "Systems of Finite Elements for Finite Bearings", ASME Journal of Lubrication Technology, pp.187-197.

Allaire, P.E. and Flack, R.D., 1981, "Design of Journal Bearings for Rotating Machinery", Proceedings of the 10th Turbomachinery Symposium, Houston, USA, pp. 25-45.

Bathe, K.J., 1982, "Finite Element Procedures in Engineering Analysis", Prentice-Hall, Englewood Cliffs, New Jersey, USA.

Booker, J.F. and Huebner, K.H., 1972, "Application of Finite Element Methods to Lubrication: An Engineering Approach", ASME Journal of Lubrication Technology, pp.313-323.

Childs, D.W., 1993, "Turbomachinery Rotordynamics: Phenomena, Modeling & Analysis", McGraw-Hill, New York, USA, 476 p.

Faria, M.T.C., Silva, L.F.A.T. and Machado, L.H.J., 2005, "Experimental Vibration and Monitoring Analysis of High-Speed Turbomachinery Using a Rotor Test Rig", Proceeding of the XIV SAE Brazil Congress, São Paulo, SAE Paper 2005-01-4017, pp. 1-7.

Faria, M.T.C., Correia, F.A.G. and Diniz, D.L.E., 2006, "Finite Element Procedure for Analysis of Oil-lubricated Cylindrical Journal Bearings" (in Portuguese), Proceedings of the XXVII Iberian Latin American Congress on Computational Methods in Engineering, Belém-PA, Brazil, pp. 1-15.

Hamrock, B.J., 1994, "Fundamentals of Fluid Film Lubrication", McGraw-Hill, New York, USA.

Huebner, K.H., Thornton, E.A. and Byrom, T.G., 1995, "The Finite Element Method for Engineers", John Wiley & Sons, 3rd Ed., New York, USA.

Juvinall, R.C. and Marshek, K.M., 1995, "Fundamentals of Machine Component Design", John Wiley & Sons, 2nd Ed., New York, USA.

Klit, P. and Lund, J.W., 1986, "Calculation of the Dynamic Coefficients of a Journal Bearing, Using a Variational Approach", ASME Journal of Tribology, Vol. 108, pp. 421-425.

Knöss, K., 1980, "Journal Bearings for Industrial Turbosets", Brown Boveri Review, Vol. 69, pp. 300-308.

Norton, R., 2000, "Machine Design – An Integrated Approach", Prentice-Hall, 2nd Ed., New York, USA.

Reddi, M.M., 1969, "Finite-Element Solution of the Incompressible Lubrication Problem", ASME Journal of Lubrication Technology, n. 3, pp. 524-533.

San Andrés, L.A., 1989, "Approximate Design of Statically Loaded Cylindrical Journal Bearings", ASME Journal of Tribology, Vol. 111, pp.390-393.

San Andrés, L.A., 1997, "Modern Hydrodynamic Lubrication Theory", class notes, Department of Mechanical Engineering, Texas A&M University, College Station, USA,

Shigley, J.E., Budynas, R.G. and Mischke, C.R., 2003, "Mechanical Engineering Design", McGraw-Hill, 7th Ed., New York, USA.

Sun, D.C., 1997, "Equations Used in Hydrodynamic Lubrication", STLE Lubrication Engineering, pp. 18-25.

Szeri, A.Z., 1980, "Tribology: Friction, Lubrication, and Wear", McGraw-Hill, New York, USA.

Szeri, A.Z., 1987, "Some Extensions of the Lubrication Theory of Osborne Reynolds", ASME Journal of Tribology, Vol. 109, n. 1, pp. 21-36.

Zeidan, F.Y. and Herbage, B.S., 1991, "Fluid Film Bearing Fundamentals and Failure Analysis", Proceedings of the 20th Turbomachinery Symposium, Houston, USA, pp. 161-186.

Zeidan, F.Y., 1992, "Developments in Fluid Film Bearing Technology", Turbomachinery International, September/October, pp.1-8.

5. RESPONSIBILITY NOTICE

The authors are the only responsible for the printed material included in this paper.